Available online at www.sciencedirect.com

ScienceDirect

Energy Procedia 44 (2014) 52 – 60

Energy Procedia

E-MRS Spring Meeting 2013 Symposium D - Advanced Inorganic Materials and Structures for Photovoltaics, 27-31 May 2013, Strasbourg, France

The Effect of Thickness on Optical Band Gap and N-type Conductivity of $CuInS_2$ Thin Films Annealed in Air Atmosphere

M. Ben Rabeh[a,*], N. Khedmi[a], M.A Fodha[a], M. Kanzari[a,b]

[a]*Laboratoire de Photovoltaïque et Matériaux Semi-conducteurs-ENIT BP 37, le Belvédère 1002-Tunis, Tunisie*

[b]*Laboratoire de Photovoltaïques et Matériaux Semi-conducteurs-ENIT-IPEITunis Montfleury-Université de Tunis*

Abstract

Structural, electrical and optical properties of $CuInS_2$ thin films of various thicknesses, grown on heated glass substrates at 100°C by thermal evaporation method were studied. These films were annealed in air atmosphere at temperature of 200°C. The thickness of the CIS films was varied from 436 to 80 nm. It was found that the structural properties, FWHM and grain size degraded with decreasing its thickness. The peak intensity decreases with the film thickness and the X-ray spectra are polycrystalline in nature excluding films with thickness less than 111nm, the peak intensity disappears and films are amorphous in nature. However, with decreasing the film thickness from 436 to 111nm, the optical band (E_g) gap of $CuInS_2$ material is in the range 1.42 to 1.81 eV. Hot probe method showed that all the annealed $CuInS_2$ samples exhibit n-type conductivity with low resistivity values in the range 3.60 to 0.08 kΩ.m. We suggests that the minimum thickness to obtain polycrystalline $CuInS_2$ thin films is 111nm, the band gap energy of $CuInS_2$ thin films can be controlled by varying the film thickness and the n-type conductivity can be obtained after annealing in air atmosphere.

Selection and peer-review under responsibility of The European Materials Research Society (E-MRS)

Keywords: $CuInS_2$; thin films; annealing; film thickness; characterization

* Corresponding author. Tel.: +216-97-442-362; fax: +216-71-921-5-98.
E-mail address: mohamedbenrabeh@yahoo.fr

doi:10.1016/j.egypro.2013.12.009

1. Introduction

A great deal of interest has been focused on the growth of the ternary I-III-VI_2 and II-IV-VI_2 semiconductor compounds which crystallize in the chalcopyrite type structure [1-4]. One of the promising chalcopyrite type semiconductors is copper indium disulfide $CuInS_2$. The ternary compound $CuInS_2$ has a direct bandgap of about 1.53 eV [5] which is nearly equal to the theoretical optimum value for photovoltaic's application. In addition, the material does not contain toxic Ga or Se atoms, and this may have an advantage in comparison with the frequently studied $CuInSe_2$ and $CuInGaS_2$. This material can be made both n and p-type, enabling the fabrication of both homo-junction and hetero-junction structures. $CuInS_2$ thin films have been deposited by various techniques, such as co-evaporation [6], molecular beam deposition [7], chemical vapour deposition [8], spray pyrolysis [9-11], chemical bath deposition [12], ion layer gas reaction [13-14] (ILGAR) and electro-deposition [15]. For controlling a conduction type and obtaining a low resistivity, several impurities doped $CuInS_2$ thin films have been also studied, such as Al, Na, O, Sn and Sb… [16-24]. T. Yamamoto et al investigated the electronic structures of n-type doped $CuInS_2$ crystals using Zn and Cd species [25]. F. Streicher et al present a comparative study of pure $CuInS_2$ (CIS) and Zn-doped $CuInS_2$ thin films using SPS in combination with a KPFM setup [26]. The sodium effect [27] has become one of the important factors affecting the energy conversion efficiency of solar cells using $CuInS_2$ thin films as absorption layers. They have demonstrated that Na incorporation into Cu-poor $CuInS_2$ thin films is essential for fabricating high efficiency $CuInS_2$-based solar cells without employing the KCN process [28]. They have also suggested that the Na incorporation annihilates the donor states generated in Na-free $CuInS_2$ films and, consequently, drastically enhanced the film conductivity, crystallite quality and device performance [29]. Also, the effect of Na doping on the optical and electrical properties of $CuInS_2$ thin films has been investigated by Zribi et al [30]. Samples were prepared by the co-evaporation of $CuInS_2$ and Na on corning 7059 glass substrates. An evolution from the n-type conductivity towards the p-type conductivity is observed. The optical band gap of the thin Na-$CuInS_2$ films decrease linearly with increasing the Na concentration. In our previous papers [18-22], we studied the effect of oxygen, tin, zinc and antimony on the structural, optical and electrical properties of $CuInS_2$ thin films grown by the thermal evaporation method. In the present work, we studied the effect of film thickness on the structural, electrical and optical properties of air annealed $CuInS_2$ thin films grown by thermal evaporation method. The process can be of interest for application in $CuInS_2$-based cell design. Therefore, the aim of this work is to convert $CuInS_2$ thin films with higher resistive to n-type conductivity and reducing the film thickness.

2. Experimental details

2.1. Synthesis

The horizontal Bridgman method is described in detail in Ref. [20]. Briefly, Cu, In and S with a nominal purity of at least 99.999% were mixed together to prepare $CuInS_2$ crystal. The mixture is introduced in an evacuated and sealed quartz tube under a vacuum of 10^{-6} Torr. The tube was inserted into the furnace where the temperature was raised to 1000°C and maintained at this temperature during 48 h. After homogenization of the melts, the tube was cooled. The obtained crystal was black color with length of 20 mm. Crushed powder of this ingot was used as raw material for the thermal evaporation to obtain $CuInS_2$ thin films.

2.2. Thin films growth

$CuInS_2$ thin films were prepared by co-evaporation of the CIS powder on glass substrates in a high vacuum system with a base pressure of 10^{-6} Torr. A tungsten crucible was used. Thermal evaporation sources were used which can be controlled either by the crucible temperature or by the source powder. The glass substrates were

heated at 100°C. After what films were annealed in air atmosphere at temperature of 200°C for 2 hours. Film thickness was measured by interference fringes method [31].

2.3. XRD

Thin films were characterized by X-ray diffraction at ambient conditions. The data were collected using a D8 Advance diffractometer in Bragg-Brentano geometry using CuKα = 1.5418 Å radiation for the phase identification and crystallographic structure.

2.4. Optical spectrophotometer

The optical transmittance and reflectance of the annealed $CuInS_2$ thin films was measured using a double-beam UV-VIS-NIR spectrophotometer (type Shimadzu UV-3100S) in the wavelength range of 300-1800 nm.

2.5. Hot probe method

The Hot-Probe method provides a simple yet efficient way to distinguish between n-type and p-type semiconductors using a heated probe and a standard multimeter. The experiment is done by attaching a couple of cold probe and hot probe to a semiconductor surface. Both probes are wired to a sensitive electrometer [32]. The hot probe is connected to the positive terminal of the meter while the cold probe is connected to the negative terminal. While applying the cold and hot probes to an n-type semiconductor, positive voltage readout is obtained in the meter, whereas for a p-type semiconductor, negative voltage is obtained [33].

3. Results and discussion

3.1. Crystallinity study

Fig. 1 shows the room temperature X-ray diffraction pattern of various air annealed $CuInS_2$ thin films with different thicknesses grown on glass substrates and measured at θ-2θ mode. It can be found that All the samples prepared with thickness equal or higher that 110 nm show strong (112) diffraction peak at 2θ = 27.8°. Also (101), (103), (004), (211) and (224) peaks with very weak intensity are observed. By cons, samples prepared with thickness less than 110 nm are amorphous in nature and the peak intensity disappears. This degradation of crystallinity can be attributed to the film thickness and indicates an increase in the disorder with decreasing thickness which may be attributed to the introduction of some defects and/or likely there is a different material forming for low thicknesses. From Fig.1, it can be seen that both the line-width and intensity of the diffraction peaks are also strongly dependent of film thickness. The inset of Fig. 1 shows dependence of the (112) peak intensity as a function of film thickness. We can see that with decreasing the film thickness, although the (112) peak intensity decrease. This reflects an improvement of the structural properties of the $CuInS_2$ when thickness is increased.

The size of the crystallites D in the grains can be estimated by the Debye-Scherrer formula [34]:

$$D = \frac{0.9 \times \lambda}{B \times \cos\theta} \quad (1)$$

Where λ is the X-ray wavelength of 1.5418Å, θ is the Bragg diffraction angle, and B is FWHM. Fig. 2 shows the dependence of FWHM value (2θ) of the diffraction peaks and the grain size, calculated from the Scherrer formula, as a function of film thickness. It can be seen that there is an increase in the FWHM and a decrease in grain size with decreasing film thickness. The FWHM increases from 0.22 to 0.63° and the grain size decreases from 37 to 13 nm rapidly, respectively, with a decreasing of annealed $CuInS_2$ film thickness. This implies that if the film thickness is reduced, this will lead to degradation in the crystallinity of the films.

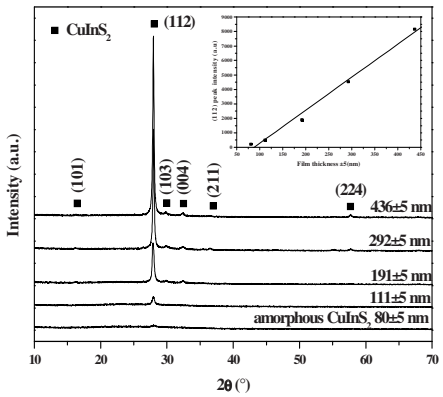

Fig. 1. X-ray diffraction pattern of air annealed $CuInS_2$ thin films grown with different thickness. The inset shows dependence of the (112) peak intensity as a function of film thickness.

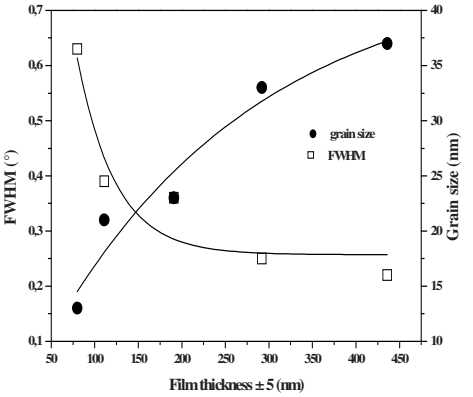

Fig. 2. The FWHM of XRD peak and film grain size vs film thickness of air annealed $CuInS_2$ thin films.

Table 1. The FWHM, grain size, resistivity and type conductivity of air annealed $CuInS_2$ thin films grown with different thickness.

Film thickness ±5 nm	FWHM (°)	Grain size (*nm*)	Resistivity $\times 10^3(\Omega m)$	Type
436	0.22	37	3.60	n
292	0.25	33	1.10	n
191	0.36	23	0.27	n
111	0.39	21	0.18	n
80	0.63	13	0.08	n

3.2. Electrical study

Several studies showed that chalcopyrite semi-conducting properties are basically governed by intrinsic native defects were donors (anion vacancies, interstitial cations) [35]. Consequently, as-deposited samples are in general highly compensated materials. This gives the opportunity to induce n-type conductivity by breaking this balance effect and to study the effect of film thickness on the n-type conductivity. We note that all the initially films are highly compensated and no specific type of conductivity was observed. To understand the effect of thickness-variation of annealed $CuInS_2$ thin films over the resistivity, we recorded the variation of the electrical resistivity as a function of temperature during the annealing in air. The resulting resistivity vs temperature curves of the fabricated $CuInS_2$ films are shown in Fig. 3.

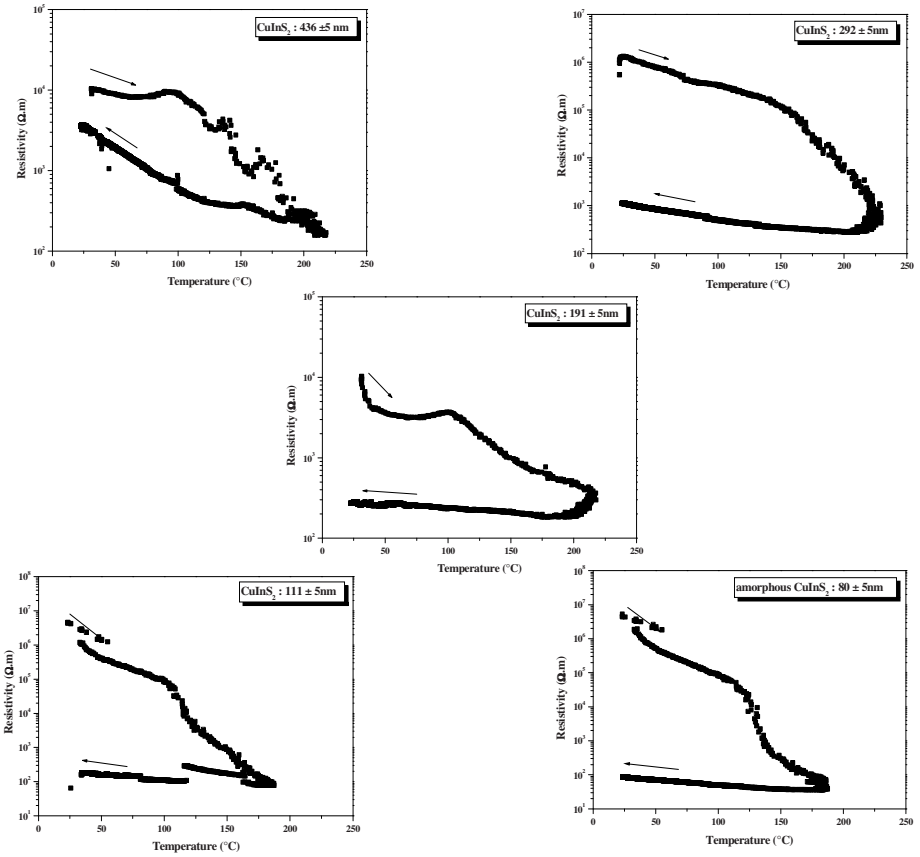

Fig. 3. Variation of electrical resistivity vs temperature of air annealed $CuInS_2$ thin films (during heating and cooling).

It is clear from the figure that after cooling by mean of hysteresis effect, all the $CuInS_2$ thin films with different thicknesses grown on glass substrates heated at 100°C do not recover their starting high resistivity values and an irreversible process was observed. This process corresponds to low resistivity in the range 3.60 to 0.18 kΩ.m with irreversible n-type conductivity. Also, we note the resistivity values deceases with decreasing film thickness, Table. 1. Which suggest improved electrical properties of samples.

3.3. Optical study

In order to analyze the effect of the film thickness on the optical properties of air annealed $CuInS_2$ thin films. The optical reflectance and transmittance spectra were investigated in the wavelength range 300-1800 nm. Figs.4 and 5 show the reflectance and transmittance spectra of air annealed $CuInS_2$ thin films grown with various

film thickness. The optical reflectance of these films varies over the range of 20-30%. Also, the transmittance increases with a decrease in the film thickness. This can be linked to the change in crystalline structure and with a decrease in the grain size and/or the density of the films.

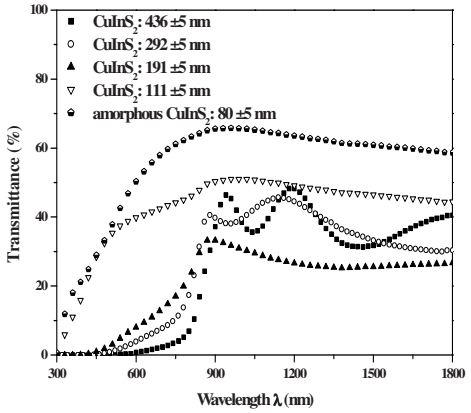

Fig. 4. Optical transmittance spectra of air annealed $CuInS_2$ thin films grown with different thickness.

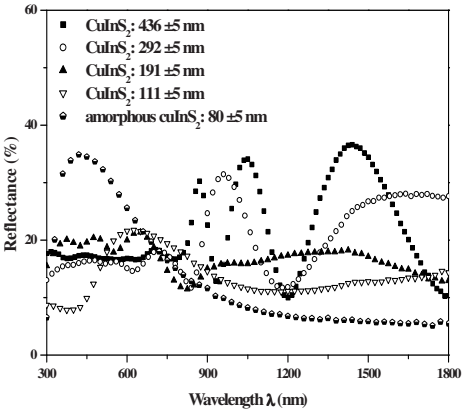

Fig. 5. Optical reflectance spectra of air annealed $CuInS_2$ thin films grown with different thickness.

The fundamental absorption corresponds to the electron excitation from valance band to conduction band and can be used to evaluate the value of the optical band gap. The optical band gap of the film is determined by applying the Tauc model, and the Davis and Mott model in the high absorbance region [36, 37]:

$$(\alpha h\nu) = A\left(h\nu - E_g\right)^n \qquad (2)$$

Here, A is a constant, hν is the photon energy, E_g is the optical band gap. For a direct transition, n=1/2 or 2/3 and the former value is more suitable for CIS film because it gives the best linear curve in the band-edge region. The absorption coefficient α (hν) of CIS thin films can be calculated from the following relation [38]:

$$\alpha = \frac{1}{d}\ln\left[\frac{\left(1-R\right)^2}{T}\right] \qquad (3)$$

Here, T is the transmittance, R is the reflectance and d is the film thickness.

Fig. 6 shows the absorption coefficients α (hν) versus the photon energy (hν) of various air annealed $CuInS_2$ thin films with different thicknesses. It can be seen that all the films have relatively high absorption coefficients between 10^4 cm^{-1} and 10^5 cm^{-1} in the visible and the near-IR spectral range. Also, we note that the absorption coefficient decreased with film thickness decreasing. Fig. 7 shows the plot of $(\alpha h\nu)^2$ vs the photon energy (hν) of various air annealed $CuInS_2$ thin films with different thicknesses varying from 436 to 80 nm. The optical band (E_g) gap first decreased, and then increased from 1.46 to 2.35 eV with film thickness decreasing, figure 8. An increase in the optical band gaps can be attributed to the film thickness [39], this behavior indicates an increase in the disorder with decreasing thickness [40] and may be attributed to the introduction of some defects which create localized states in the band-gap and therefore increase the band-gap [40]. Similar results were also observed by other researchers [39, 40]. These results suggest that the optical band gap of $CuInS_2$ thin films can be controlled more precisely by controlling the thickness CIS films. It is also known that the thickness becomes important in the

thin films. The thickness of the film causes a shift in the optical absorption edge and therefore a change in the band structure of the films. It is found that the optical absorption edge varies with increasing film thickness. This suggests that the defects in thin films occur during the formation of the films.

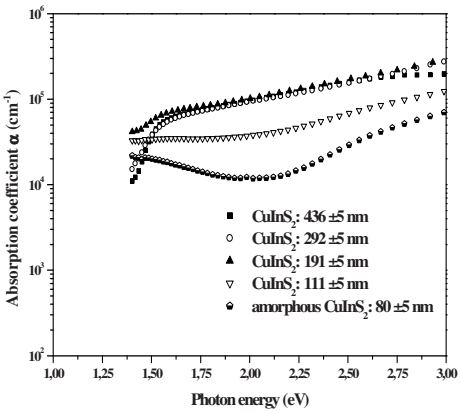

Fig. 6. Absorption coefficient spectra of air annealed $CuInS_2$ thin films grown with different thickness.

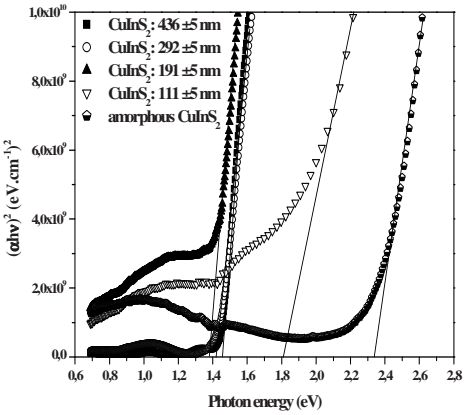

Fig. 7. The plot of $(\alpha h\nu)^2$ vs $(h\nu)$ of air annealed $CuInS_2$ thin films grown with different thickness.

Thus, unsatured bonds can be produced as a result of an insufficient number of atoms [41]. These bonds are responsible for the formation of some defects in the films and these defects produce localized states in the films. The thicker film increases the width of localized states in the optical band gap, consequently, the optical absorption edge decreases with the reverse effect [39].

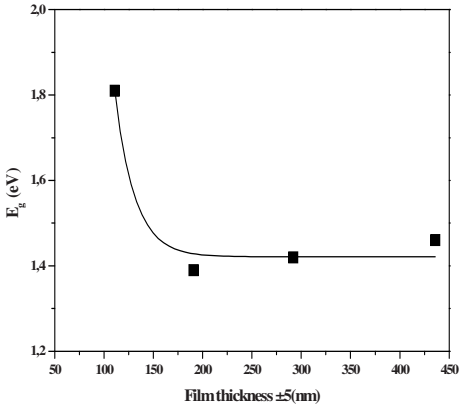

Fig. 8. Variation of band gap energy E_g vs film thickness of air annealed $CuInS_2$ thin films.

4. Conclusion

The structural, electrical and optical properties of air annealing $CuInS_2$ thin films grown with different thickness were studied. The thickness of the CIS films was varied from 436 to 80 nm. We have found a change between physical properties and air annealing of CIS films in term of thickness. The structural properties degraded the FWHM increases from 0.22° to 0.36° and the grain size decreases from 37 to 13 nm with decreasing film

thickness. The peak intensity decreases with the film thickness and the X-ray spectra are polycrystalline in nature excluding films with thickness less than 110nm, the peak intensity disappears and films are amorphous in nature. The minimum thickness to obtain polycrystalline $CuInS_2$ thin films is 111nm. The optical band (E_g) gap first decreased, and then increased from 1.42 to 1.80 eV. The resistance values decreased from 3.60 to 0.08 kΩ.m with film thickness decreased. All the annealed films exhibit n-type conductivity. Thus, film thickness in $CuInS_2$ plays very important role in band gap energy controlling and air annealing leads to n-type conductivity.

References

[1] Iseler GW, Kildal H, Menyuk N. Ternary compounds: Institute of Physics Conference Series 35. London; 1977.
[2] Kazmerski LI. Ternary compounds: Institute of Physics Conference Series 35; 1977.
[3] Romeo N. Ternary and multinary compounds; Proceedings of the 4th international conference. Japanese Journal of Applied Physics 1980;19:5-133.
[4] Wagner S, Bridenbaugh PM. Multicomponent tetradral compounds for solor cells. Journal of Crystal Growth 1977;39:151-159.
[5] Shay JL, Tell B, Kasper HM, Schiavone LM. p-d Hybridation of the valence bands of I-III-VI_2 compounds. Physical Review B 1972;5:5003-5005.
[6] Bandyopadhyaya S, Chaudhuri S, Pal AK. Synthesis of $CuInS_2$ films by sulphurization of Cu/In stacked elemental layers. Solar Energy Materials and Solar Cells 2000;60: 323-339.
[7] Gossla M, Hahn T, Metzner H, Conrad J, Geyer U. Thin $CuInS_2$ films by 3-source molecular-beam deposition. Thin Solid Films 1995;268:39-44.
[8] Hollingsworth JA, Banger KK, Jin MH-C, Harris JD, Cowen JE, Bohannan EW, Switzer JA, Buhro WE, Hepp AF. Single source precursors for fabrication of I-III-VI_2 thin film solar cells via spray CVD. Thin Solid Films 2003;431-432:63-67.
[9] Ortega-Lopez M, Morales-Acevedo A. Characterization of $CuInS_2$ thin films for solar cells prepared by spray pyrolysis. Thin Solid Films 1998;330: 96-101.
[10] Tiwari AN, Pandya DK, Chopra KL. Electrical and optical properties of single-phase $CuInS_2$ films prepared using spray pyrolysis. Thin Solid Films 1985;130:217-230.
[11] Krunks M, MiKli V, Bijakina O, Rebane H, Mere A, Varema T, Mellikov E. Composition and structure of $CuInS_2$ films prepared by spray pyrolysis. Thin Solid Films 2000; 361– 362:61-64.
[12] Mahmoud S, Eid AH. Some studies on chemically and thermally prepared $CuInS_2$ films. Fizika A 1997;6:171-180.
[13] Möller J, Fischer CH-H, Muffler HJ, Könenkamp R, Kaiser I, Kelch C, Lux-Steiner MC. A novel deposition technique for compound semiconductors on highly porous substrates: ILGAR. Thin Solid Films 2000; 361-362:113-117.
[14] Muffler H-J, Fischer Ch-H, Diesner K, Lux-Steiner MC. ILGAR-A novel thin-film technology for sulphides. Solar Energy Materials and Solar Cells 2001;67:121-127.
[15] Yukawa T, Kuwabara K, Koumoto K. Electrodeposition of $CuInS_2$ from aqueous solution (II) electrodeposition of $CuInS_2$ film. Thin Solid Films 1996;286:151-153.
[16] Allouche N Kamoun, Jebbari N, Guasch C, Turki NKamoun. Ifluence of aluminium doping in $CuInS_2$ prepared by spray pyrolysis on different substrates. Journal of Alloys and Compounds 2010;501:85-88.
[17] John TT, Sebastian T, Kartha CS, Vijayakumar KP, Abe T, Kashiwaba Y. Effects of incorporation of Na in spray pyrolysed $CuInS_2$ thin films. Physica B: Condensed Matter 2007;388: 1-9.
[18] Ben Rabeh M, Kanzari M, Rezig B. Role of oxygen in enhancing N-type conductivity of $CuInS_2$ thin films. Thin Solid Films 2007;515:5943-5948.
[19] Ben Rabeh M, Zribi M, Kanzari M, Rezig B. Structural and optical characterization of Sn incorporation in $CuInS_2$ thin films grown by vacuum evaporation method. Materials Letters 2005;59:3164-3168.
[20] Ben Rabeh M, Chaglabou N, Kanzari M. Effect of antimony incorporation on structural properties of $CuInS_2$ crystals. Nuclear Instruments and Methods in Physics Research B 2010;268:273-276.
[21] Zribi M, Ben Rabeh M, Brini R, Kanzari M, Rezig B. Influence of Sn incorporation on the properties of $CuInS_2$ thin films grown by vacuum evaporation method. Thin Solid Films 2006;511-512:125-129.
[22] Ben Rabeh M, Kanzari M, Rezig B. Effect of Zinc Incorporation in $CuInS_2$ thin films grown by vacuum evaporation method. Acta Physica Polonica A 2009;115: 699-703.
[23] Zribi M, Kanzari M, Rezig B. Post-growth annealing treatment effects on properties of Na-doped $CuInS_2$ thin films. Materials Science and Engineering B 2008;149:1-6.
[24] Zribi m, Kanzari m, Rezig B. Optical constants of Na-doped $CuInS_2$ thin films. Materials Letters 2006;60: 98-103.
[25] Streicher F, Sadewasser S, Enzenhofer T, Schock HW, Lux-Steiner M Ch. Locally resolved surface photo voltage spectroscopy on Zn-doped $CuInS_2$ polycrystalline thin films. Thin Solid Films 2009;517: 2349-2352.
[26] Yamamoto T, V Luck IIka, Scheer R. Materials design of n-type CuInS2 thin films using Zn or Cd species. Applied Surface Science 2000;159-160:350-354.
[27] Watanabe T, Nakazawa H, Matsui M, Ohbo H, Nakada T. The influence of sodium on the properties of $CuInS_2$ thin films and solar cells. Solar Energy Materials and Solar Cells 1997;49:357-363.
[28] Watanabe T, Yamamoto T. Control of defects in $CuInS_2$ thin films by incorporation of Na and O. Japanese Journal of Applied Physics 2000;39:1280-1282.
[29] Watanabe T, Nakazawa H, Matsui M. Improvement of the electrical properties of Cu-poor $CuInS_2$ thin films by sodium incorporation. Japanese Journal of Applied Physics 1998;37:1370-1372.

[30] Zribi M, Kanzari M, Rezig B. Effects of Na incorporation in $CuInS_2$ thin films. The European Physical Journal Applied Physics 2005;29:203-207.
[31] Heavens O.S. Optical Properties of Thin Solid Films; Butterworths: London; 1950.
[32] B. Van Zeghbroeck. Principales of electronic devices:Principle of Semiconductor Devices;1997.
[33] Golan G, Axelevitch A, Gorenstein B, Manevych V. Hot-probe method for evaluation of impurities cpncentration in semiconductors. Microelectronics Journal 2006;37:910–915.
[34] Klug HP, Alexander LE. X-ray Diffraction Procedures for Polycrystalline and Amorphous Materials. Wiley-Interscience. New York; 1974.p.594-597.
[35] Hulliger F, Mooser E.The bond description of semiconductors: polycompounds. Progress in Solid State Chemistry 1965;2:330-377.
[36] Tauc J. Amorphous and Liquid Semiconductors. Plenum Press. London; 1974.
[37] David EA, Mott NF. Conduction in non-crystalline systems V. Conductivity, optical absorption and photoconductivity in amorphous semiconductors. Philosophical Magazine 1970;22:903-922.
[38] Milovzorov DE, Ali AM, Inokuma T, Kurata Y, Suzuki T, Hasegawa S. Optical properties of silicon nanocrystallites in polycrystalline silicon films prepared at low temperature by plasma –enhanced chemical vapour deposition. Thin Solid Films 2001;382: 47-55.
[39] Sönmezoğlu S, Arslan A, Serin T, Serin N. The effects of film thickness on the optical properties of TiO_2-SnO_2 compound thin films. Physica Scripta 2011;84:065602-065607.
[40] Varnamkhasti MG, Fallah HR, Mostajaboddavati M, Hassanzadeh A. Influence of Ag thickness on electrical, optical and structural properties of nanocrystalline MoO_3/Ag/ITO multilayer for optoelectronic applications. Vacuum 2012;86:1318-1322.
[41] Ovshinsky SR, Adler D. Local structure, bonding, and electronic properties of covalent amorphous semiconductors. Contemporary Physics 1978;19:109-126.